Article

Mechanosensitive Oligodithienothiophenes: Transmembrane Anion Transport Along Chalcogen-Bonding Cascades

MACCHIONE, Mariano, *et al*.

Abstract

The design, synthesis, and evaluation of multifunctional dithieno[3,2-b;2′,3′-d]thiophene (DTT) trimers is described. Twisted push-push-pull or donor-donor-acceptor (DDA) trimers composed of one DTT acceptor and two DTT donors show strong mechanochromism in lipid bilayer membranes. Red shifts in excitation rather than emission and fluorescence recovery with increasing membrane order are consistent with planarization of the twisted, extra-long mechanophores in the ground state. The complementary pull-pull-pull or AAA trimers with deep σ holes all along the scaffold are not mechanochromic in membranes but excel with submicromolar anion transport activity. Anion transport along membrane-spanning strings of chalcogen-bond donors is unprecedented and completes previous results on transmembrane cascades that operate with equally unorthodox interactions such as halogen bonds and anion-π interactions.

Reference

MACCHIONE, Mariano, *et al*. Mechanosensitive Oligodithienothiophenes: Transmembrane Anion Transport Along Chalcogen-Bonding Cascades. *Helvetica Chimica Acta*, 2018, vol. 101, no. 4, p. e1800014

DOI : 10.1002/hlca.201800014

Mechanosensitive Oligodithienothiophenes: Transmembrane Anion Transport Along Chalcogen-Bonding Cascades

Mariano Macchione, Maria Tsemperouli, Antoine Goujon, Ajith R. Mallia, Naomi Sakai, Kaori Sugihara, and Stefan Matile*

School of Chemistry and Biochemistry, National Centre of Competence in Research (NCCR) Chemical Biology, University of Geneva, Quai Ernest Ansermet 30, 1211 Geneva 4, Switzerland, e-mail: stefan.matile@unige.ch

Dedicated to *François Diederich* on the occasion of his retirement

The design, synthesis, and evaluation of multifunctional dithieno[3,2-*b*;2′,3′-*d*]thiophene (DTT) trimers is described. Twisted push-push-pull or donor-donor-acceptor (DDA) trimers composed of one DTT acceptor and two DTT donors show strong mechanochromism in lipid bilayer membranes. Red shifts in excitation rather than emission and fluorescence recovery with increasing membrane order are consistent with planarization of the twisted, extra-long mechanophores in the ground state. The complementary pull-pull-pull or AAA trimers with deep σ holes all along the scaffold are not mechanochromic in membranes but excel with submicromolar anion transport activity. Anion transport along membrane-spanning strings of chalcogen-bond donors is unprecedented and completes previous results on transmembrane cascades that operate with equally unorthodox interactions such as halogen bonds and anion-π interactions.

Keywords: chalcogen bonds, ion transport, dithienothiophenes, oligomers, mechanophores, fluorescent probes.

Introduction

The creation of synthetic transport systems has attracted scientific attention since decades.[1 – 11] This fascination originates from the importance of ion transport across lipid bilayer membranes in biology and the molecular complexity, variability, and beauty with which this most challenging process is achieved. Until today, there is much interest in transport mechanisms, particularly synthetic ion channels but also mobile carriers and transporters.[2 – 11] However, since the appearance of the first operational systems, ion selectivity and particularly the responsiveness to physical and chemical stimulation emerged as key challenges in the field. Because of its significance in biology, voltage gating received much attention early on.[12 – 15] Elegant examples exist for control of synthetic ion channels by pH and light, including artificial photosystems.[1] Most recent breakthroughs concern progress toward ion pumps, *i.e.*, active transport,[16][17] as well as mechanosensitive synthetic ion channels.[18] With regard to chemical stimulation, ligand gating and blockage, *i.e.*, the activation and inhibition of synthetic transport systems by molecular recognition, are of highest importance.[19 – 21] Extension of these themes toward sensing[22][23] and particularly catalysis,[24] that is molecular transformation on the way across lipid bilayer membranes, remain intriguing and still surprisingly underdeveloped.

Privileged scaffolds for the construction of synthetic transport systems include rod-shaped oligomers, helical foldamers, π stacks, macrocycles such as cyclodextrins, crown ethers, pillararenes, calixarenes, cucurbiturils or G quartets, small monomers such as steroids and large architectures including metallorganic polyhedrons and DNA origami.[1 – 24]

The contact between synthetic transport systems and cations is usually established by coordination to lone pairs, whereas hydrogen bond donors are mostly used to transport anions.[1 – 24] Cation-π interactions have been introduced as an attractive alternative at a time when they were still considered to account also for potassium selectivity in neural channels.[25] The hopping of cations along ligand-assembled bundles of membrane-spanning strings of π-basic arenes, occurred indeed with selectivity sequences similar to those found in nature (*Figure 1,d*). The complementary π slides composed of three π-acidic naphthalenediimides

DOI: 10.1002/hlca.201800014 *Helv. Chim. Acta* **2018**, *101*, e1800014

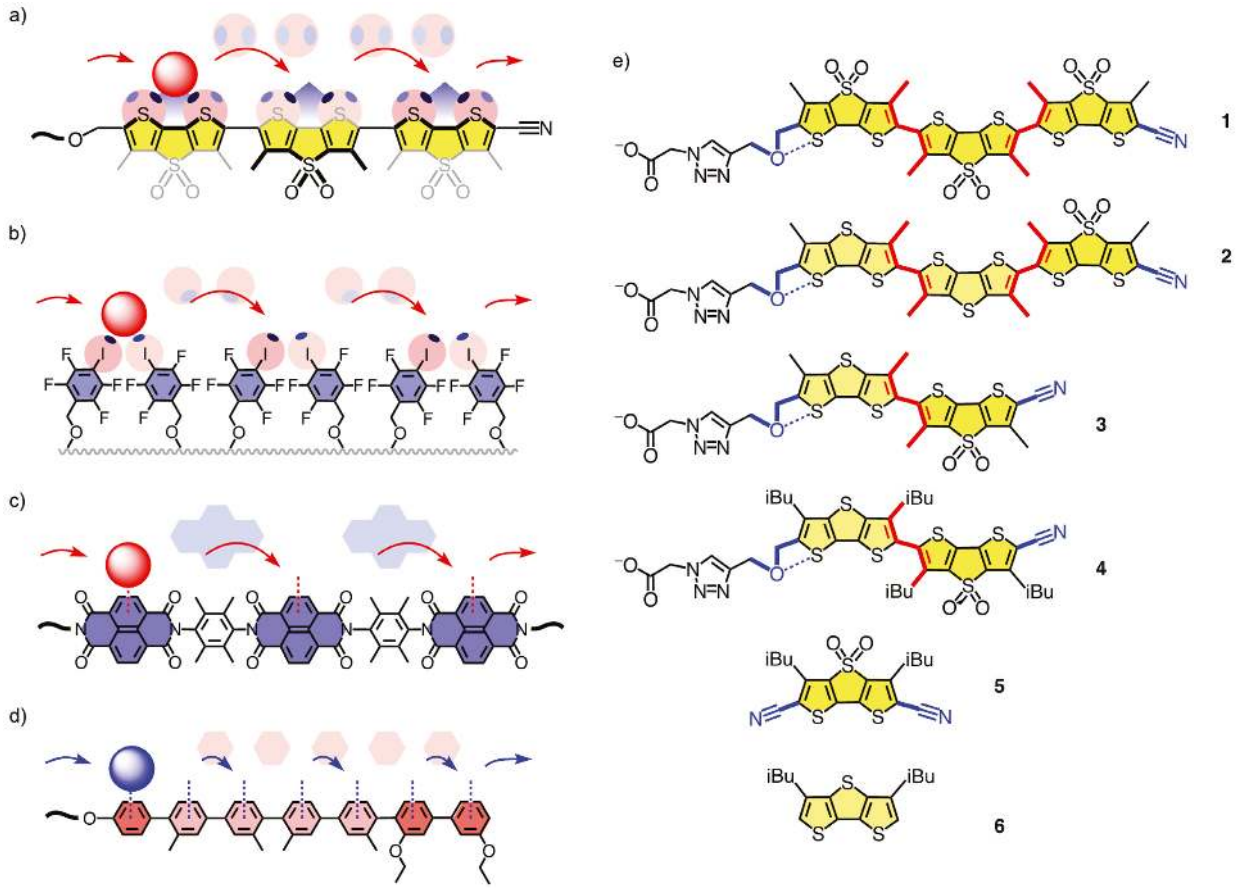

Figure 1. Schematic anion hopping along transmembrane strings of chalcogen-bond donors *a*) compared to the previously realized halogen-bonding *b*), anion-π *c*) and cation-π slides *d*). Red: Electron rich, blue: Electron poor, red circles: Anions (*e.g.* Cl^-), blue circles: Cations (*e.g.* K^+). Self- or ligand-gated assembly into confirmed or expected channel-like transmembrane bundles is indicated schematically. *e*) Structure of chalcogen-bonding anion transporters used in this study.

caused the expected inversion from cation to anion selectivity (*Figure 1,c*).[26] The promise of anion-π interactions in synthetic transport systems has since been validated in many variations, also with very small systems, and extended to catalysis.[27 – 29]

As a second unorthodox alternative to anion transport with hydrogen bonds, halogen bonds[30][31] appeared particularly attractive because they are more hydrophobic and more directional. These expectations have been confirmed with the discovery of the smallest possible organic anion transporter, trifluoroiodomethane, and expansion to transmembrane halogen-bonding cascades provided access to very high activities (*Figure 1,b*).[32] Moving from halogen to chalcogen bonds, anion transport has been demonstrated recently with small monomers.[33] In this report, we complete this series with the synthesis and evaluation of a small collection of dithieno[3,2-*b*:2′,3′-*d*]thiophene (DTT)[34 – 36] oligomers **1** – **6** for anion transport along transmembrane chalcogen-bonding cascades of different length and strength (*Figure 1,a,* and *1,e*).

Chalcogen bonds originate from the σ holes that appear on increasingly electron-deficient sulfur, selenium, tellurium but not oxygen atoms.[37][38] Associated with anti-bonding σ^* orbitals, chalcogen bonds from σ hole donors extend linearly from the two covalent bonds (*Figure 1,a*). Presumably because the σ holes are somewhat hidden on the side of the donor atom, the use of chalcogen bonds has been mostly limited to solid state engineering and extensive intramolecular covalent conformational control, particularly in medicinal chemistry.[37 – 41] Pioneering recent examples for intermolecular chalcogen bonds include macrocycles,[42] rotaxanes,[43] and anion binding.[43][44]

In 2016, we have introduced DTTs as a privileged motif to integrate intermolecular chalcogen bonds into functional systems in solution.[33] Molecular models confirmed that the bite angle is ideal to bind anions in the focal point of the two σ holes of the cofacial, conformationally immobilized endocyclic sulfur atoms (*Figure 1,a*). This motif thus offers for chalcogen bonds what bipyridine lone pairs offer for cation

binding and bipyrroles for anion binding with hydrogen bonds. Anion transport[33] and catalytic[45 – 48] activities increased with increasing depth of the σ holes in electron-deficient DTTs such as **5** compared to **6**.

Dimeric DTTs **3** have been introduced in the same year as mechanosensitive fluorescent membrane probes.[49] They represent the last step in the evolution of planarizable push-pull probes.[49 – 54] Chalcogen-bond repulsion between methyls and σ holes is introduced to twist the two DTTs out of co-planarity. The push-pull system is established with formal sulfide donors and sulfone acceptors in the central ring of the tricyclic DTTs, the latter supported by an exocyclic cyano acceptor. The 'ETC headgroup' is composed of an ether donor, a triazole base to prevent elimination and a carboxylate to assure delivery to and orientation in lipid bilayer membranes.[49] As anionic amphiphiles, DTTs **3** form non-fluorescent micelles in water and partition into membranes as monomers with their scaffold, according to depth quenching studies, aligned to the lipid tails and the anionic carboxylate at the membrane surface.[49 – 54] Mechanical planarization of the twisted push-pull probe **3** in the ground state causes the excitation maxima to shift to the red. This differs conceptually from other membrane probes that operate by deplanarization (molecular rotors), polarization (solvatochromism) and electron or proton transfer in the excited state and thus report in emission rather than excitation.[55 – 68] The resulting flipper probes **3** are important because they provide access to the so far elusive imaging of forces such as membrane tension in living cells (unpublished). Overtwisting in dimeric DTTs **4** results in a total loss of mechanosensitivity.[69]

In this report, we move on from functional DTT monomers (anion transport) and dimers (mechanophores) and report the design, synthesis and evaluation of trimeric DTTs **1** and **2**. The pull-pull-pull or acceptor-acceptor-acceptor (AAA) trimer **1** aligns three electron-deficient S,S-dioxide DTTs to produce transmembrane strings of deep σ holes for anion transport along chalcogen-bonding cascades. The push-push-pull or donor-donor-acceptor (DDA) trimer **2** offers two DTT donors next to a DTT acceptor to strengthen the push-pull system and thus maximize the mechanosensitivity of the longest flipper probe made so far.

Results and Discussion

Lessons learned with monomers and dimers[33][49 – 53][69] made the synthesis of the twisted AAA and DDA trimers **1** and **2** conceivable (*Scheme 1*). The starting point for both was tetrabromothiophene **7**. Following reported procedures, the DTT scaffold was obtained from the elegant cascade reaction with thioacetate **8** and acetaldehyde **9**.[69] Hydrolysis and decarboxylation of diester **10** gave dimethyl DTT **11**, which was readily formylated to give aldehyde **12** as the first, previously reported[51] but differently prepared key intermediate. Aldehyde **12** was first oxidized to the brightly fluorescent DTT S,S-dioxide **13** and then reduced to alcohol **14**, which was silyl protected to afford key intermediate **15** for further use. The same aldehyde **12** was further brominated to **16**, which was converted to cyano DTT **17** and oxidized to afford DTT S,S-dioxide **18**, another important intermediate, ready for *Stille* coupling with the unsubstituted dimethyl DTT **11**. The resulting DTT dimer **19** was first brominated to **20** and then oxidized to the S,S-dioxide **21**. *Stille* coupling with DTT S,S-dioxide **15** provided access to the trimeric scaffold **22** with three fully oxidized DTT S,S-dioxides. This twisted AAA trimer **22** was then processed following the methods developed on the dimer level.[49] Namely, deprotection with fluoride gave alcohol **23**, etherification with the bromide **24** gave alkyne **25**, and CuAAC with azide **26** afforded the complete scaffold **27**, which was thoroughly purified in this hydrophobic form before deprotection under basic conditions to yield the desired AAA amphiphile **1**.

Aldehyde **12** was also the starting point for the synthesis of the complementary DDA trimer **2** (*Scheme 2*). Reduction of the aldehyde gave the primary alcohol **28**, which was protected with a silyl group. *Stille* coupling of the resulting monomer **29** with dimer **20** afforded trimer **30** with the desired push-pull scaffold. From this DDA trimer **30**, the synthesis of **2** was finalized as described above for the fully oxidized analog **22**. Namely, deprotection with fluoride followed by alkylation of the primary alcohol **31** with bromide **24**, CuAAC of alkyne **32** with azide **26** and final deprotection of ester **33** afforded the target molecule **2**. As for AAA amphiphile **1** and contrary to all hydrophobic precursors including **33**, the very low solubility in all solvents of DDA amphiphile **2** hindered routine characterization beyond ^{1}H-NMR spectroscopy in deprotonated form in (D_6)DMSO/D_2O (1.5 M ND_4OD) 9:1. Dimers **3** and **4** and monomers **5** and **6** were prepared as described previously. Details on the synthesis and characterization of all new compounds can be found in the *Supporting Information*.

The spectroscopic properties of the new AAA and DDA trimers **1** and **2** were mostly determined with their hydrophobic precursors **22** and **30**, respectively, because the final amphiphiles were poorly soluble in

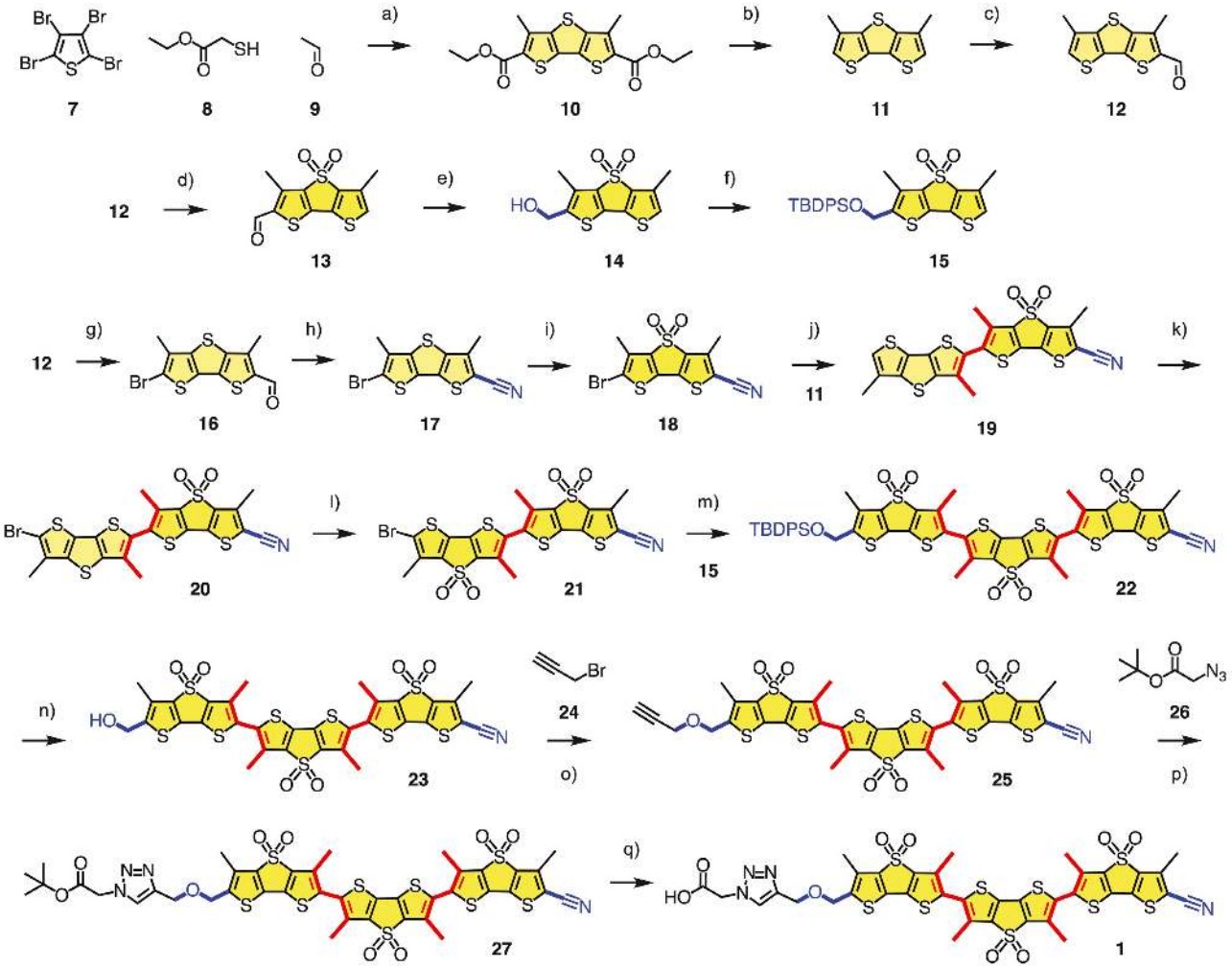

Scheme 1. *a*) 1. **7**, BuLi, THF, −78 °C, **9**, 45 min, 2. $Na_2Cr_2O_7$, H_2SO_4, H_2O, acetone, r.t., 16 h, 3. EtONa, EtOH, **8**, reflux, 1 h, 80%; *b*) 1. LiOH, EtOH, reflux, 16 h, 2. Ag_2CO_3, AcOH, DMSO, 120 °C, 16 h, 69%; *c*) $POCl_3$, DMF, 50 °C, 2 h, 75%;[51] *d*) mCPBA, $CHCl_3$, 37 °C, 16 h, 72%; *e*) DIBAL-H, CH_2Cl_2, −78 °C to r.t., 1 h; *f*) imidazole, TBDPSCl, NEt_3, DMF, r.t., 16 h, 50%; *g*) NBS, DMF, 80 °C, 24 h, 80%;[51] *h*) NaN_3, TfOH, MeCN, 82 °C, 4 h, 70%;[52] *i*) mCPBA, CH_2Cl_2, r.t., 12 h, 65%;[52] *j*) 1. **11**, BuLi, Bu_3SnCl, THF, −78 °C to r.t., 1 h, 2. **18**, $Pd(PPh_3)_4$, toluene, 80 °C, 48 h, 72%; *k*) NBS, CH_2Cl_2, 40 °C, 1.5 h, 86%; *l*) mCPBA, CH_2Cl_2, 40 °C, 1.5 h, 62%; *m*) 1. **15**, BuLi, Bu_3SnCl, THF, −78 °C to r.t., 45 min, 2. **21**, $Pd(PPh_3)_4$, DMF, 80 °C, 30 h, 53%; *n*) TBAF, AcOH, THF, r.t., 15 min; *o*) NaH, THF, −20 °C to r.t., 16 h, 15% (2 steps); *p*) $CuSO_4 \cdot 5\ H_2O$, sodium ascorbate, TBTA, CH_2Cl_2/H_2O 4:1, r.t., 15 min, 58%; *q*) KOH, CH_2Cl_2/MeOH 1:1, r.t., 10 min, 98%. mCPBA = 3-Chloroperbenzoic acid; TBDPS = *tert*-Butyldiphenylsilyl; TBTA = Tris[(1-benzyl-1*H*-1,2,3-triazol-4-yl)methyl]amine; TfOH = Trifluoromethansulfonic acid.

apolar solvents. Consistent with decreasing fluorescence with increasing oligomer length, *i.e.*, rotatable bonds,[54] fluorescence quantum yields decreased dramatically from the hydrophobic precursors of DA dimer **3** to trimers **2** and particularly **1** (*Table 1*). In AcOEt, absorption and emission maxima of the hydrophobic AAA **22** and DDA **30** were overall not significantly red shifted compared to hydrophobic precursors of dimers **3** and **4** (*Figure 2*, *Table 1*). Compared to AAA trimer **22**, the absorption maximum of DDA trimer **30** was blue shifted (from λ_{abs} = 420 nm to λ_{abs} = 360 nm), whereas the emission maximum shifted to the red (from λ_{em} = 560 nm to λ_{em} = 590 nm). These shifts with DDA **30** were as expected for an increasing twist between electron-rich monomers in the ground state and an increasing dipole of the push-pull system in the planar excited state. Interestingly, the absorption maximum of DDA trimer **30** was much broader than that of the AAA trimer **22**. The distinct shoulder appearing red-shifted from the maximum at λ_{abs} = 360 nm could indicate the occurrence of partial planarization of the highly

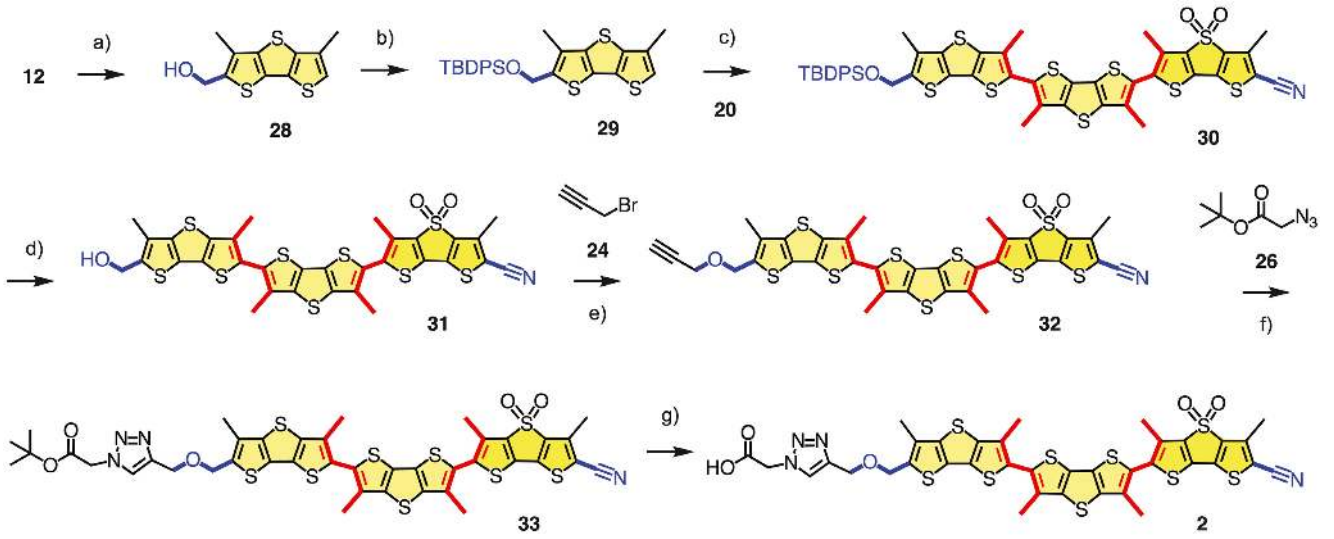

Scheme 2. *a*) $NaBH_4$, DMF, 70 °C, 2 h; *b*) imidazole, TBDPSCl, DMF, r.t., 12 h, 70% (2 steps);[51] *c*) 1. **29**, BuLi, Bu_3SnCl, THF, −78 °C to r.t., 45 min, 2. **20**, $Pd(PPh_3)_4$, toluene, 75 °C, 16 h, 74%; *d*) TBAF, AcOH, THF, r.t., 30 min; *e*) NaH, THF, 0 °C to r.t., 16 h, 59% (2 steps); *f*) $CuSO_4 \cdot 5\ H_2O$, sodium ascorbate, TBTA, CH_2Cl_2/H_2O 4:1, r.t., 15 min, 56%; *g*) KOH, CH_2Cl_2/MeOH 1:1, r.t., 15 min, 98%.

twisted ground state already in low-viscosity bulk AcOEt solution.

Twisted ground states and operational push-pull dipoles in the planar excited states were consistent with little solvatochromism in excitation but strong positive solvatochromism in emission spectra (*Figure 2*). According to *Lippert* analysis,[50 – 54] the variation of the permanent dipole moment upon excitation increased from $\Delta\mu$ = 13.4 D for the less polarized AAA trimer **22** to $\Delta\mu$ = 17.9 D for the more polarized DDA trimer **30** (*Table 1*). Whereas increasing $\Delta\mu$ with bulkier α substituents from the hydrophobic precursors of **3** to **4** on the dimer level was consistent with the onset of excited-state deplanarization (*i.e.*, TICT, twisted intramolecular charge transfer),[69] increasing $\Delta\mu$ from AAA **22** to DDA **30** on the trimer level occurred with identical bulk but increasing polarization. This polarization thus originated presumably from increased ICT in a planarized, fully conjugated push-pull excited state. This interpretation was in agreement with strong mechanochromism of the twisted DDA trimer **2** but not the less polarized AAA trimer **1** in lipid bilayer membranes (below).

Like their dimeric homologs,[49 – 53][69] trimers **1** and **2** did not fluoresce in water (*Figure 3,a*, red). Addition of 0.5 μM of DDA trimer **2** to large unilamellar vesicles (LUVs) composed of dipalmitoyl-*sn*-glycero-

Table 1. Ion transport and spectroscopic characteristics of DTT monomers, dimers, and trimers[a]

Compound[b]	EC_{50} (transport) [μM][c]	$\Delta\lambda_{ex}$[d] (ΔI)[e]	$\Delta\mu$ (D)[f]	λ_{abs}[g] (ε)[h]	λ_{em}[i] (ϕ)[j]
1	0.28 ± 0.05	–	13.4	420 (24.7)	560 (1.8)
2	3.5 ± 0.3	+40 (3.2)	17.9	360 (37.7)	590 (2.7)
3	4.0 ± 0.3	+70[k][l] (2.7)	13.6[l]	413 (18.9)[l]	570 (31)[l]
4	7.8 ± 1.7	~0 (~1)[m]	14.8[m]	409 (18.7)[m]	610 (4.4)[m]
5	1.9 ± 0.2[n]	nd	nd	376 (18.3)[n]	440 (20)
6	16 ± 3[n]	nd	nd	nd	nd

[a] For original data and conditions, see *Figures 2 – 4* and *Supporting Information*. [b] Compounds, see *Figure 1*. [c] Transport activity: Effective concentration needed to reach 50% of maximal activity in the HPTS assay; from *Hill* analysis of dose response curves (*Figure 4,a* and *4,b*). [d] Mechanosensitivity: Wavelength λ_{ex} (in nm) at excitation maximum in DPPC LUVs at 25 °C minus λ_{ex} in DPPC LUVs at 55 °C; [e] intensity I at λ_{ex} in DPPC LUVs at 25 °C divided by I at λ_{ex} in DPPC LUVs at 55 °C (*Figure 3,b*). [f] Transition dipole: Variation of the permanent dipole moment upon excitation (in Debye); from *Lippert* analysis of solvatochromism (*Figure 2*). [g] Wavelength λ_{abs} (in nm) at absorption maximum in AcOEt. [h] Extinction coefficient (in $mM^{-1}\ cm^{-1}$) at λ_{abs}. [i] Wavelength λ_{em} (in nm) at emission maximum in AcOEt. [j] Fluorescence quantum yield (in %) in air-saturated AcOEt. [f – j] Measured with hydrophobic precursors of the final amphiphiles, *i.e.*, **22** instead of **1** and **30** instead of **2**. [k] Broad maximum in DPPC at 25 °C, $\Delta\lambda_{ex}$ = +50 to +90 nm. [l] From ref. [49]. [m] From ref. [69]. [n] From ref. [33].

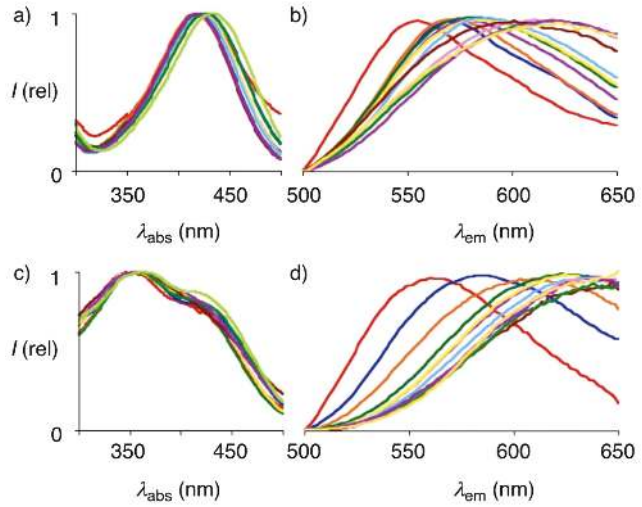

Figure 2. Normalized absorption (*a*, *c*) and emission spectra (*b*, *d*, excitation at λ_{abs}) of hydrophobic precursors of (*a*, *b*) AAA trimer **1** (*i.e.*, **22**) and (*c*, *d*) DDA trimer **2** (*i.e.*, **30**) in hexane (red), toluene (blue), Et_2O (orange), $CHCl_3$ (violet), AcOEt (green), THF (yellow), CH_2Cl_2 (light blue), acetone (pink), MeOH (brown), DMF (green), MeCN (purple), DMSO (yellow).

3-phosphocholine (DPPC) in liquid-disordered (L_d) phase at 55 °C caused an instantaneous fluorescence recovery with λ_{ex} = 440 nm (*Figure 3,a* and *3,b*). Cooling down into solid-ordered (S_o) DPPC membranes at 25 °C red shifted the excitation maximum to λ_{ex} = 480 nm and increased the fluorescence intensity by a factor of $\Delta I = I_{S_o}/I_{L_d}$ = 3.2 (*Figure 3,b*, *Table 1*).

Control experiments in dioleoyl-*sn*-glycero-3-phosphocholine (DOPC) LUVs confirmed that these changes do not originate from thermochromism. Namely, with DOPC membranes in L_d phase at 55 °C and 25 °C, the excitation maxima were nearly identical. Moreover, the emission maximum λ_{em} = 575 nm was essentially insensitive to changes from S_o to L_d phase, confirming that contributions from other mechanisms like solvatochromism[55 – 68] do not account for the observed changes in excitation (*Figure 3,f*). According to lessons learned from dimeric flipper probes including DA homolog **3**, the response in excitation of the elongated trimeric DDA probe **2** to increasing order in the surrounding membrane originates from planarization in the ground state, *i.e.*, mechanosensitivity (*Figure 3, c*). The impressive shift of $\Delta\lambda_{ex}$ = +80 nm from λ_{ex} = 360 nm of the fully relaxed flipper in organic solvents to λ_{ex} = 440 nm suggested that significant planarization already occurs in L_d membranes (*Figure 3,e*). The additional shift $\Delta\lambda_{ex}$ = +40 nm from L_d to S_o membranes to λ_{ex} = 480 nm was consistent with further ground-state planarization with increasing membrane order (*Figure 3,b, 3,c,* and *3,e*, *Table 1*).

Compared to $\Delta\lambda_{ex}$ = +70 nm from L_d membranes to a broad maximum around λ_{ex} = 485 nm in S_o membranes of dimeric push-pull flipper **3**,[49] the $\Delta\lambda_{ex}$ = +40 nm to λ_{ex} = 480 nm of the trimeric homolog **2** failed to further improve mechanochromism (*Table 1*). The fluorescence recovery ΔI = 3.2 upon planarization from L_d to S_o membranes of trimer **3** exceeded the ΔI = 2.7 of dimer **2** (*Figure 3,b*, *Table 1*). This could originate from the immobilization of more rotatable bonds and would be of interest for imaging in cells by FLIM (Fluorescence lifetime imaging microscopy). However, the poor quantum yield ϕ = 2.7% in AcOEt clearly excluded any practical use of push-pull DDA trimer **2** for imaging within[70][71] and on the surface of cells, although it will increase substantially upon planarization in membranes of increasing order.

Because of the very low quantum yield, the fluorescence spectra of AAA trimer **1** in DPPC LUVs could not be recorded. The only possible indication for mechanochromism of AAA trimer **1** was obtained from the orange color in solution and the deep red color of AAA precursor **22** as a solid (*Figure 3,d*). However, the interpretation of this impressive red shift as ground-state planarization should be met with caution because other possible origins of color change in the solid state cannot be excluded. Poor mechanosensitivity of pull-pull dimers was noted earlier.[51]

Whereas mechanosensitive fluorescence in membranes was thus reserved for the planarizable DDA trimer **2**, ion transport activity was better with the strongest chalcogen-bonding cascade offered by AAA trimer **1** (*Figure 1,a*). Transport activities were determined in large unilamellar vesicles (LUVs) composed of egg yolk phosphatidylcholine (EYPC) and loaded with the ratiometric pH-sensitive probe HPTS (8-hydroxy-1,3,6-pyrenetrisulfonate). To these vesicles, a pH gradient was applied with a base pulse (*Figure 4, a**). The dissipation of this pH gradient was then measured after addition of the transporters (*Figure 4,a***). At the end of each experiment, excess gramicidin D was added to calibrate the fluorescence response against the resulting maximal fractional activity Y_{total} (*Figure 4,a****). Dose response curves were recorded at constant vesicle concentration to determine the effective concentration EC_{50} of transporters needed to reach 50% of the maximal accessible activity Y_{max} with excess transporter (*Figure 4,b*).

The transport activity of the chalcogen-bonding cascade in AAA trimer **1** was outstanding: A submicromolar EC_{50} = 0.28 ± 0.05 μM is traditionally very difficult to achieve, a $Y_{max} \approx 1$ as well (*Figure 4,a,* and *4, b●*, *Table 1*). Similarly powerful transport has been observed for membrane-spanning halogen-bonding

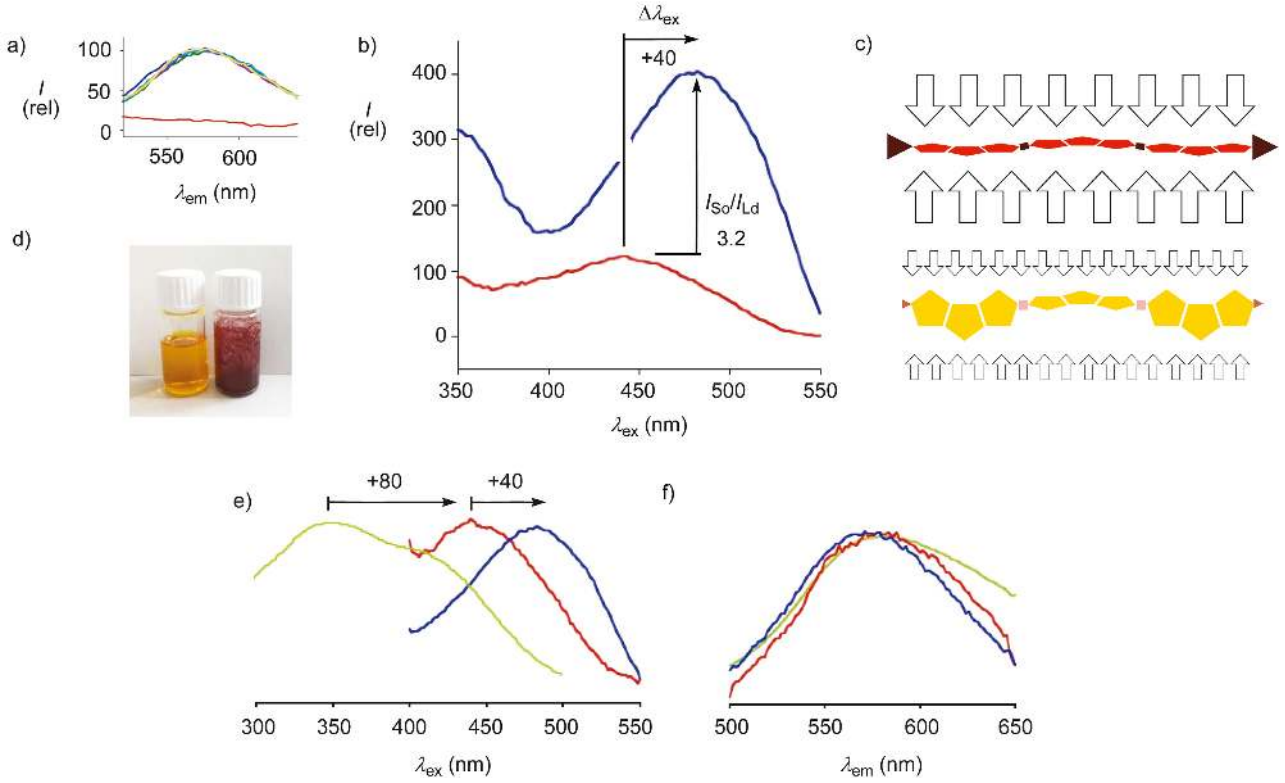

Figure 3. *a*) In-scale, not normalized fluorescence emission spectra of 0.5 μM **2** in buffer before (red) and 1, 5, 10, 15, and 30 min after the addition to DPPC LUVs at 55 °C (λ_{ex} = 440 nm). *b*) In-scale, not normalized fluorescence excitation spectra of 0.5 μM **2** in DPPC LUVs at 55 °C (red) and 25 °C (λ_{em} = 575 nm). *c*) Schematic planarization of twisted push-pull trimers in environments of increasing order. *d*) Fully oxidized trimer **22** in AcOEt (orange) and in the solid state (deep purple). *e, f*) Comparison of normalized fluorescence (*e*) excitation and (*f*) emission spectra of hydrophobic precursor **30** in AcOEt (light green) and amphiphile **2** in DPPC LUVs at 55 °C (red) at 25 °C (blue).

cascades (*Figure 1,b*), but not for shorter halogen-bonding transporters.[32] Push-pull DDA trimer **2** of equal length but with deep σ holes only on one S,S-dioxide DTT monomer failed to reach submicromolar activity, with EC_{50} = 3.5 ± 0.3 μM (*Figure 4,b*○, *Table 1*). Moreover, the highest achievable activity $Y \sim 0.5$ indicated delivery problems at higher concentrations, presumably due to poor solubility in micellar form in water (*Figure 4,b*○).

It was interesting to find that oligomers **2** – **4** were all more than ten times less active than AAA trimer **1**, and that their activity did not differ much (*Table 1*, *entries 2 – 4*). This trend suggested that the isolate deep σ holes near the outer surface are all that matters for anion transport, whereas length and twist of the scaffold extending into the membrane are much less important. The transmembrane string of deep σ holes in **1** thus accounts presumably for the high activity of AAA trimer **1**. In monomer **5**, this single chalcogen-bonding site is unchained from the membrane surface and allowed to shuttle freely across the membrane (*Table 1*, *entry 5*). The result was an appreciable increase in anion transport activity down to EC_{50} = 1.9 ± 0.2 μM. However, the expected movement of the A monomer **5** with the anion across the membrane remained clearly less effective than the expected movement of anions along the immobile cascade of anion binding sites offered by the outstanding AAA trimer **1**. In D monomer **6** with a disappointing EC_{50} = 16 ± 3 μM, high mobility did not suffice to produce high activity because the σ holes are too shallow to strongly bind anions.[33] This poor activity with shallow σ holes nicely illustrated why DDA trimer **2** failed to establish an operational transmembrane chalcogen-bonding cascade although the length of the scaffold is as in AAA trimer **1**. Although all trends thus provided a good match between structure and activities in support of the power of operational chalcogen-bonding cascades, it is important to reiterate that other explanations can never be fully excluded in experiments of this complexity, and that all interpretations should be considered with appropriate caution.

The exchange of external anions affected activities more than the exchange of external cations

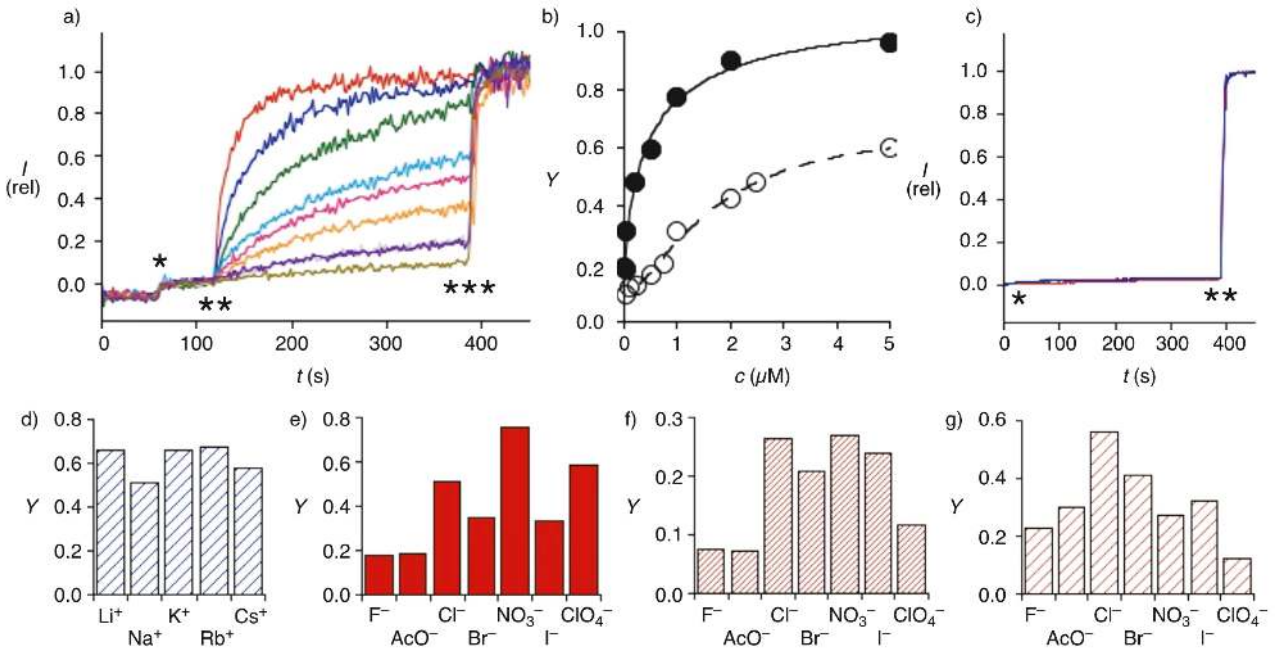

Figure 4. *a*) Ratiometric change in emission intensity *I* (λ_{em} = 510 nm, λ_{ex} = 450/405 nm) with time *t* during the application of a base pulse (*, 20 μL 0.5 M NaOH) followed by the addition of **1** (**, 20 μL DMSO stock solution to 2 mL, final concentrations = 0.01, 0.02, 0.05, 0.2, 0.5, 1, 2, 5 μM (with increasing activity)), and excess gramicidin D (***) to egg yolk phosphatidylcholine (EYPC) vesicles with intravesicular HPTS. *b*) Dependence of the fractional transport activity *Y* in the HPTS assay (*a*) on the concentration *c* of AAA trimer **1** (●) and DDA trimer **2** (○). *c*) Change in emission intensity *I* (λ_{ex} = 492 nm, λ_{em} = 517 nm) with time *t* during the addition of **1** and **2** (*, 0.5 and 1.7 μM, respectively) and excess triton X-100 (**) to EYPC vesicles with internal, self-quenched 5(6)-carboxyfluorescein (CF). *d-g*) Dependence of the activity *Y* of AAA trimer **1** (*d, e*), DDA trimer **2** (*f*) and A monomer **5** (*g*)[33] in the HPTS assay (*a*) on the variation of extravesicular cations (*d*, 100 mM MCl, inside 100 mM NaCl) and anions (*e* – *g*, 100 mM NaX, inside 100 mM NaCl).

(*Figure 4,d* – *4,g*). Interestingly, the apparent anion selectivity sequences were the same only for halides ($Cl^- > Br^- \sim I^- > F^-$), whereas the activities of oxyanions ($NO_3^- > ClO_4^-$) relative to halides increased from the mobile chloride carrier **5**[33] to the apparent nitrate transporters **2** and particularly **1** (*Figure 4,e* – *4,g*). Although the origin of these trends can be complex, direct comparison with conductivity experiments[72][73] support that the observed anion selectivities originate either from proton-anion symport or from hydroxide-anion antiport. For antiport, initial, 'invisible' exchange of the varied external anions with internal chloride should be fast because of the applied gradients and the large excess of the former.[26] The increase of intravesicular pH reported by HPTS would then occur by hydroxide influx and coinciding efflux of the previously imported variable anion, present in large excess. Inactivity in control experiments with vesicles reporting on the efflux of CF, a large fluorescent anion, confirmed that the new transporters do not form large pores (*Figure 4,c*). The observed anion selectivity was consistent with operational chalcogen-bonding cascades (*Figure 1, a*). The high activity with oxyanions of the best performing AAA trimer **1** could indicate selective recognition in transmembrane bundles. The geometry and the larger distance between the recognized lone pairs compared to halides possibly allowed for better anion hopping along the focal points of deep σ holes of DTT S,S-dioxides triads across the lipid bilayer membrane.

The most active AAA trimer **1** was active also in planar bilayer conductance experiments (*Figure 5*). Addition to *cis* chamber separated from *trans* chamber by an insulating POPC membrane yielded transmembrane currents (*Figure 5,a*). Their stepwise appearance was more similar to resolved single-channel currents obtained with α-hemolysin[74] (*Figure 5,c*) than to the unresolved macroscopic currents produced by ion carrier valinomycin[75] (*Figure 5,d*). Although we observed current steps that indicate pore formation, the conductance from the pores *g* ranged from 0.16 nS to 1.40 nS (corresponding to the pore diameter *d* of 2.3 – 7.0 Å, based on the *Hille* equation),[76 – 78] which suggested that, not unexpectedly, there is no particular stable pore size (*Figure 5,b*).

These channel currents at various conductance supported the self-assembly of AAA trimer **1** into transmembrane bundles, with different numbers of monomers per bundle possibly accounting for the different single channel currents. The stepwise opening of the large conductance in *Figure 5,b* could reflect

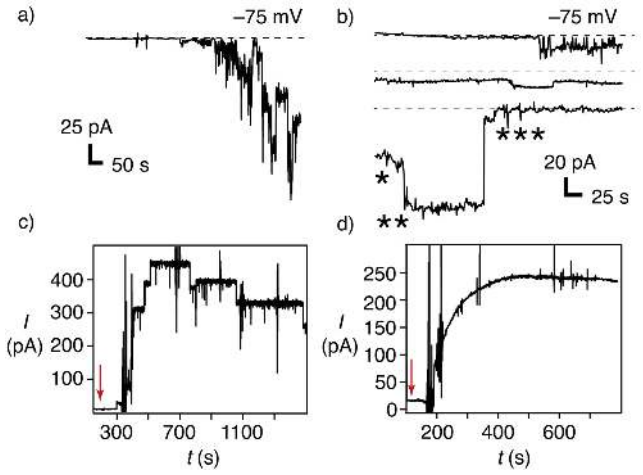

Figure 5. Planar bilayer conductance in the presence of *a*) AAA trimer **1** (50 μM added to *cis* chamber with POPC membranes) at −75 mV (*trans* as ground) in 2 M KCl *cis* and *trans*, compared to the signatures of α-hemolysin (*c*) and valinomycin (*d*); red arrows indicate the moment, where each compound was added to the chamber. *b*) Representative single-channel currents in the presence of AAA trimer **1**. *Opening of a channel; **expansion of the channel size or opening of a second channel; ***closing or diffusion of the channel out of the planar bilayer area.

either the expansion of the pore size during the measurement by incorporating more **1** in the bundle or opening of a spontaneous second pore in the planar bilayer (from *Figure 5,b** to *5,b***), followed by closing or the diffusion of the pore/pores out of the planar bilayer area into the annulus, where organic solvent dysfunctions the channel structure (*Figure 5,b****). Although similar bundle expansions and contractions have been studied in detail with, for example, the α-helical ion channel alamethicin,[79] these interpretations are of course highly speculative and made with the only intention to illustrate possible explanations.

Conclusions

The objective of this study was to move from multifunctional DTT monomers and dimers to trimers. Two complementary trimers were designed, synthesized and evaluated, *i.e.*, push-pull trimers composed of one DTT acceptor and two DTT donors and chalcogen-bonding trimers with deep σ holes all along the scaffold.

The planarizable push-pull trimers excel with strong solvatochromism in solution. Large red shifts in excitation upon ground-state planarization already in liquid-disordered membranes confirm unprecedented mechanosensitivity. Further red shifts from liquid-disordered to solid-ordered membranes are correspondingly smaller compared to the homologous dimers. Fluorescence recovery upon ground-state planarization is better with the new trimers than with the old dimers. Compared to dimeric flipper probes, planarizable push-pull trimers would thus be of interest to image properties between the two leaflets of lipid bilayer membranes. Their poor fluorescence is however incompatible with use in practice.

The complementary trimers with a cascade of deep σ holes instead of a strong push-pull dipole along the twisted scaffold excel with submicromolar anion transport activity rather than mechanochromism. Increasing anion transport with increasing number of deep σ holes along the scaffold provides strong support that anion transport occurs along transmembrane chalcogen-bonding cascades. This unprecedented activity and selectivity obtained with chalcogen bonds compare favorably to transmembrane cascades operating with halogen bonds[32] and anion-π interactions.[26] The twisted, asymmetric scaffold of chalcogen-bonding trimers promises access to an exceptionally rich multifunctionality, including mechanosensitive channels,[18] pumps (active transport),[16] electroneutral photosystems,[80] and catalytic pores.[24] Studies along these lines are ongoing, together with synthetic efforts toward higher DTT oligomers, tetramers and beyond.

Experimental Section

See *Supplementary Material*.

Supplementary Material

Supporting information for this article is available on the WWW under https://doi.org/10.1002/hlca.201800014.

Acknowledgements

We thank the NMR and MS platforms for services, and the *University of Geneva*, the *Swiss National Centre of Competence in Research (NCCR) Chemical Biology*, the *NCCR Molecular Systems Engineering* and the *Swiss NSF* for financial support.

Author Contribution Statement

M. M., *N. S.*, and *S. M.* conceived this work; *M. M.*, *A. G.*, and *A. R. M.* synthesized the compounds, *M. M.*, *M. T.*, *N. S.*, *K. S.*, and *S. M.* designed the experiments; *M. M.* and *M. T.* conducted the experiments; all authors discussed the results and commented on the manuscript, *M. M.*, *M. T.*, *N. S.*, *K. S.*, and *S. M.* wrote the manuscript.

References

[1] N. Sakai, S. Matile, 'Synthetic Ion Channels', *Langmuir* **2013**, *29*, 9031 – 9040.

[2] J. E. Jones, V. Diemer, C. Adam, J. Raftery, R. E. Ruscoe, J. T. Sengel, M. I. Wallace, A. Bader, S. L. Cockroft, J. Clayden, S. J. Webb, 'Length-Dependent Formation of Transmembrane Pores by 3_{10}-Helical α-Aminoisobutyric Acid Foldamers', *J. Am. Chem. Soc.* **2016**, *138*, 688 – 695.

[3] M. Lisbjerg, H. Valkenier, B. M. Jessen, H. Al-Kerdi, A. P. Davis, M. Pittelkow, 'Biotin[6]uril Esters: Chloride-Selective Transmembrane Anion Carriers Employing C-H···Anion Interactions', *J. Am Chem. Soc.* **2015**, *137*, 4948 – 4951.

[4] S. Schneider, E.-D. Licsandru, I. Kocsis, A. Gilles, F. Dumitru, E. Moulin, J. Tan, J.-M. Lehn, N. Giuseppone, M. Barboiu, 'Columnar Self-Assemblies of Triarylamines as Scaffolds for Artificial Biomimetic Channels for Ion and for Water Transport', *J. Am. Chem. Soc.* **2017**, *139*, 3721 – 3727.

[5] C. Ren, J. Shen, H. Zeng, 'Combinatorial Evolution of Fast-Conducting Highly Selective K^+ Channels via Modularly Tunable Directional Assembly of Crown Ethers', *J. Am. Chem. Soc.* **2017**, *139*, 12338 – 12341.

[6] S. V. Shinde, P. Talukdar, 'A Dimeric Bis(melamine)-Substituted Bispidine for Efficient Transmembrane H^+/Cl^- Cotransport', *Angew. Chem. Int. Ed.* **2017**, *56*, 4238 – 4242.

[7] M. Boccalon, E. Iengo, P. Tecilla, 'Metal-Organic Transmembrane Nanopores', *J. Am. Chem. Soc.* **2012**, *134*, 20310 – 20313.

[8] P. A. Gale, J. T. Davis, R. Quesada, 'Anion Transport and Supramolecular Medicinal Chemistry', *Chem. Soc. Rev.* **2017**, *46*, 2497 – 2519.

[9] E. N. W. Howe, N. Busschaert, X. Wu, S. N. Berry, J. Ho, M. E. Light, D. D. Czech, H. A. Klein, J. A. Kitchen, P. A. Gale, 'pH-Regulated Nonelectrogenic Anion Transport by Phenylthiosemicarbazones', *J. Am. Chem. Soc.* **2016**, *138*, 8301 – 8308.

[10] J. Kempf, A. R. Schmitzer, 'Metal-Organic Synthetic Transporters (MOST): Efficient Chloride and Antibiotic Transmembrane Transporters', *Chem. Eur. J.* **2017**, *23*, 6441 – 6451.

[11] J. R. Burns, K. Göpfrich, J. W. Wood, V. V. Thacker, E. Stulz, U. F. Keyser, S. Howorka, 'Lipid-Bilayer-Spanning DNA Nanopores with a Bifunctional Porphyrin Anchor', *Angew. Chem. Int. Ed.* **2013**, *52*, 12069 – 12072.

[12] T. M. Fyles, D. Loock, X. Zhou, 'A Voltage-Gated Ion Channel Based on a Bis-Macrocyclic Bolaamphiphile', *J. Am. Chem. Soc.* **1998**, *120*, 2997 – 3003.

[13] C. Goto, M. Yamamura, A. Satake, Y. Kobuke, 'Artificial Ion Channels Showing Rectified Current Behavior', *J. Am. Chem. Soc.* **2001**, *123*, 12152 – 12159.

[14] N. Sakai, S. Matile, 'Recognition of Polarized Lipid Bilayers by *p*-Oligophenyl Ion Channels: From Push-Pull Rods to Push-Pull Barrels', *J. Am. Chem. Soc.* **2002**, *124*, 1184 – 1185.

[15] J.-Y. Winum, S. Matile, 'Rigid Push-Pull Oligo(*p*-phenylene) Rods: Depolarization of Bilayer Membranes with Negative Membrane Potential', *J. Am. Chem. Soc.* **1999**, *121*, 7961 – 7962.

[16] G. Su, M. Zhang, W. Si, Z.-T. Li, J.-L. Hou, 'Directional Potassium Transport Through a Unimolecular Peptide Channel', *Angew. Chem. In. Ed.* **2016**, *55*, 14678 – 14682.

[17] W. Si, P. Xin, Z.-T. Li, J.-L. Hou, 'Tubular Unimolecular Transmembrane Channels: Construction Strategy and Transport', *Acc. Chem. Res.* **2015**, *48*, 1612 – 1619.

[18] T. Muraoka, K. Umetsu, K. V. Tabata, T. Hamada, H. Noji, T. Yamashita, K. Kinbara, 'Mechano-Sensitive Synthetic Ion Channels', *J. Am. Chem. Soc.* **2017**, *139*, 18016 – 18023.

[19] N. Sakai, B. Baumeister, S. Matile, 'Transmembrane B-DNA', *ChemBioChem* **2000**, *1*, 123 – 125.

[20] V. Gorteau, F. Perret, G. Bollot, J. Mareda, A. N. Lazar, A. W. Coleman, D.-H. Tran, N. Sakai, S. Matile, 'Synthetic Multifunctional Pores with External and Internal Active Sites for Ligand Gating and Noncompetitive Blockage', *J. Am. Chem. Soc.* **2004**, *126*, 13592 – 13593.

[21] T. Muraoka, T. Endo, K. V. Tabata, H. Noji, S. Nagatoishi, K. Tsumoto, R. Li, K. Kinbara, 'Reversible Ion Transportation Switch by a Ligand-Gated Synthetic Supramolecular Ion Channel', *J. Am. Chem. Soc.* **2014**, *136*, 15584 – 15595.

[22] S. Hagihara, H. Tanaka, S. Matile, 'Boronic Acid Converters for Reactive Hydrazide Amplifiers: Polyphenol Sensing in Green Tea with Synthetic Pores', *J. Am. Chem. Soc.* **2008**, *130*, 5656 – 5657.

[23] T. Takeuchi, J. Montenegro, A. Hennig, S. Matile, 'Pattern Generation with Synthetic Sensing Systems in Lipid Bilayer Membranes', *Chem. Sci.* **2011**, *2*, 303 – 307.

[24] B. Baumeister, N. Sakai, S. Matile, '*p*-Octiphenyl beta-Barrels with Ion Channel and Esterase Activity', *Org. Lett.* **2001**, *3*, 4229 – 4232.

[25] M. M. Tedesco, B. Ghebremariam, N. Sakai, S. Matile, 'Modeling the Selectivity of Potassium Channels with Synthetic, Ligand-Assembled π-Slides', *Angew. Chem. Int. Ed.* **1999**, *38*, 540 – 543.

[26] V. Gorteau, G. Bollot, J. Mareda, S. Matile, 'Rigid-Rod Anion–π Slides for Multiion Hopping Across Lipid Bilayers', *Org. Biomol. Chem.* **2007**, *5*, 3000 – 3012.

[27] X. Zheng, L. Liu, J. López-Andarias, C. Wang, N. Sakai, S. Matile, 'Anion-π Catalysis: Focus on Nonadjacent Stereocenters', *Helv. Chim. Acta* **2018**, *101*, e1700288.

[28] J. López-Andarias, A. Frontera, S. Matile, 'Anion-π Catalysis on Fullerenes', *J. Am. Chem. Soc.* **2017**, *139*, 13296 – 13299.

[29] Y. Cotelle, V. Lebrun, N. Sakai, T. R. Ward, S. Matile, 'Anion-π Enzymes', *ACS Cent. Sci.* **2016**, *2*, 388 – 393.

[30] O. Dumele, B. Schreib, U. Warzok, N. Trapp, C. A. Schalley, F. Diederich, 'Halogen-Bonded Supramolecular Capsules in the Solid State, in Solution, and in the Gas Phase', *Angew. Chem. Int. Ed.* **2017**, *56*, 1152 – 1157.

[31] G. Cavallo, P. Metrangolo, R. Milani, T. Pilati, A. Priimagi, G. Resnati, G. Terraneo, 'The Halogen Bond', *Chem. Rev.* **2016**, *116*, 2478 – 2601.

[32] A. Vargas Jentzsch, S. Matile, 'Transmembrane Halogen-Bonding Cascades', *J. Am. Chem. Soc.* **2013**, *135*, 5302 – 5303.

[33] S. Benz, M. Macchione, Q. Verolet, J. Mareda, N. Sakai, S. Matile, 'Anion Transport with Chalcogen Bonds', *J. Am. Chem. Soc.* **2016**, *138*, 9093 – 9096.

[34] M. E. Cinar, T. Ozturk, 'Thienothiophenes, Dithienothiophenes, and Thienoacenes: Syntheses, Oligomers, Polymers, and Properties', *Chem. Rev.* **2015**, *115*, 3036 – 3140.

[35] G. Barbarella, F. Di Maria, 'Supramolecular Oligothiophene Microfibers Spontaneously Assembled on Surfaces or

Coassembled with Proteins Inside Live Cells', *Acc. Chem. Res.* **2015**, *48*, 2230 – 2241.
[36] A. Mishra, C. Ma, P. Bäuerle, 'Functional Oligothiophenes: Molecular Design for Multidimensional Nanoarchitectures and their Applications', *Chem. Rev.* **2009**, *109*, 1141 – 1276.
[37] B. R. Beno, K.-S. Yeung, M. D. Bartberger, L. D. Pennington, N. A. Meanwell, 'A Survey of the Role of Noncovalent Sulfur Interactions in Drug Design', *J. Med. Chem.* **2015**, *58*, 4383 – 4438.
[38] A. Bauzá, T. J. Mooibroek, A. Frontera, 'The Bright Future of Unconventional σ/π-Hole Interactions', *ChemPhysChem* **2015**, *16*, 2496 – 2517.
[39] H. Huang, L. Yang, A. Facchetti, T. J. Marks, 'Organic and Polymeric Semiconductors Enhanced by Noncovalent Conformational Locks', *Chem. Rev.* **2017**, *117*, 10291 – 10318.
[40] J. Fanfrlík, A. Přáda, Z. Padělková, A. Pecina, J. Macháček, M. Lepšík, J. Holub, A. Růžička, D. Hnyk, P. Hobza, 'The Dominant Role of Chalcogen Bonding in the Crystal Packing of 2D/3D Aromatics', *Angew. Chem. Int. Ed.* **2014**, *53*, 10139 – 10142.
[41] A. Kremer, A. Fermi, N. Biot, J. Wouters, D. Bonifazi, 'Supramolecular Wiring of Benzo-1,3-chalcogenazoles through Programmed Chalcogen Bonding Interactions', *Chem. Eur. J.* **2016**, *22*, 5665 – 5675.
[42] P. C. Ho, P. Szydlowski, J. Sinclair, P. J. W. Elder, J. Kübel, C. Gendy, L. M. Lee, H. Jenkins, J. F. Britten, D. R. Morim, I. Vargas-Baca, 'Supramolecular Macrocycles Reversibly Assembled by Te-O Chalcogen Bonding', *Nat. Commun.* **2016**, *7*, 11299.
[43] J. Y. C. Lim, I. Marques, A. L. Thompson, K. E. Christensen, V. Felix, P. D. Beer, 'Chalcogen Bonding Macrocycles and [2]Rotaxanes for Anion Recognition', *J. Am. Chem. Soc.* **2017**, *139*, 3122 – 3133.
[44] G. E. Garrett, G. L. Gibson, R. N. Straus, D. S. Seferos, M. S. Taylor, 'Chalcogen Bonding in Solution: Interactions of Benzotelluradiazoles with Anionic and Uncharged Lewis Bases', *J. Am. Chem. Soc.* **2015**, *137*, 4126 – 4133.
[45] S. Benz, J. López-Andarias, J. Mareda, N. Sakai, S. Matile, 'Catalysis with Chalcogen Bonds', *Angew. Chem. Int. Ed.* **2017**, *56*, 812 – 815.
[46] P. Wonner, L. Vogel, M. Düser, L. Gomes, F. Kniep, B. Mallick, D. B. Werz, S. M. Huber, 'Carbon–Halogen Bond Activation by Selenium-Based Chalcogen Bonding', *Angew. Chem. Int. Ed.* **2017**, *56*, 12009 – 12012.
[47] S. Benz, J. Mareda, C. Besnard, N. Sakai, S. Matile, 'Catalysis with Chalcogen Bonds: Neutral Benzodiselenazole Scaffolds with High-Precision Selenium Donors of Variable Strength', *Chem. Sci.* **2017**, *8*, 8164 – 8169.
[48] S. Benz, A. I. Poblador-Bahamonde, N. Low-Ders, S. Matile, 'Catalysis with Pnictogen, Chalcogen, and Halogen Bonds', *Angew. Chem. Int. Ed.* https://doi.org/10.1002/anie.201801452.
[49] S. Soleimanpour, A. Colom, E. Derivery, M. Gonzalez-Gaitan, A. Roux, N. Sakai, S. Matile, 'Headgroup Engineering in Mechanosensitive Membrane Probes', *Chem. Commun.* **2016**, *52*, 14450 – 14453.
[50] B. Baumeister, S. Matile, 'Rigid-Rod β-Barrels as Lipocalin Models: Probing Confined Space by Carotenoid Encapsulation', *Chem. Eur. J.* **2000**, *6*, 1739 – 1749.
[51] M. Dal Molin, Q. Verolet, A. Colom, R. Letrun, E. Derivery, M. Gonzalez-Gaitan, E. Vauthey, A. Roux, N. Sakai, S. Matile, 'Fluorescent Flippers for Mechanosensitive Membrane Probes', *J. Am. Chem. Soc.* **2015**, *137*, 568 – 571.
[52] Q. Verolet, M. Dal Molin, A. Colom, A. Roux, L. Guénée, N. Sakai, S. Matile, 'Twisted Push-Pull Probes with Turn-On Sulfide Donors', *Helv. Chim. Acta* **2017**, *100*, e1600328.
[53] Q. Verolet, A. Rosspeintner, S. Soleimanpour, N. Sakai, E. Vauthey, S. Matile, 'Turn-On Sulfide π Donors: An Ultrafast Push for Twisted Mechanophores', *J. Am. Chem. Soc.* **2015**, *137*, 15644 – 15647.
[54] D. Alonso Doval, M. Dal Molin, S. Ward, A. Fin, N. Sakai, S. Matile, 'Planarizable Push-Pull Oligothiophenes. In Search of the Perfect Twist', *Chem. Sci.* **2014**, *5*, 2819 – 2825.
[55] A. S. Klymchenko, 'Solvatochromic and Fluorogenic Dyes as Environment-Sensitive Probes: Design and Biological Applications', *Acc. Chem. Res.* **2017**, *50*, 366 – 375.
[56] T. Baumgart, G. Hunt, E. R. Farkas, W. W. Webb, G. W. Feigenson, 'Fluorescence Probe Partitioning between L_o/L_d Phases in Lipid Membranes', *Biochim. Biophys. Acta – Biomembranes* **2007**, *1768*, 2182 – 2194.
[57] I. A. Karpenko, M. Collot, L. Richert, C. Valencia, P. Villa, Y. Mély, M. Hibert, D. Bonnet, A. S. Klymchenko, 'Fluorogenic Squaraine Dimers with Polarity-Sensitive Folding as Bright Far-Red Probes for Background-Free Bioimaging', *J. Am. Chem. Soc.* **2015**, *137*, 405 – 412.
[58] I. López-Duarte, P. Chairatana, Y. Wu, J. Pérez-Moreno, P. M. Bennett, J. E. Reeve, I. Boczarow, W. Kaluza, N. A. Hosny, S. D. Stranks, R. J. Nicholas, K. Clays, M. K. Kuimova, H. L. Anderson, 'Thiophene-Based Dyes for Probing Membranes', *Org. Biomol. Chem.* **2015**, *13*, 3792 – 3802.
[59] L. A. Bagatolli, 'To See or Not to See: Lateral Organization of Biological Membranes and Fluorescence Microscopy', *Biochim. Biophys. Acta – Biomembranes* **2006**, *1758*, 1541 – 1556.
[60] E. Sezgin, F. Betul Can, F. Schneider, M. P. Clausen, S. Galiani, T. A. Stanly, D. Waithe, A. Colaco, A. Honigmann, D. Wüstner, F. Platt, C. Eggeling, 'A Comparative Study on Fluorescent Cholesterol Analogs as Versatile Cellular Reporters', *J. Lipid Res.* **2016**, *57*, 299 – 309.
[61] M. K. Kuimova, 'Mapping Viscosity in Cells using Molecular Rotors', *Phys. Chem. Chem. Phys.* **2012**, *14*, 12671 – 12686.
[62] X. Peng, Z. Yang, J. Wang, J. Fan, Y. He, F. Song, B. Wang, S. Sun, J. Qu, J. Qi, M. Yan, 'Fluorescence Ratiometry and Fluorescence Lifetime Imaging: Using a Single Molecular Sensor for Dual Mode Imaging of Cellular Viscosity', *J. Am. Chem. Soc.* **2011**, *133*, 6626 – 6635.
[63] Z. Yang, Y. He, J.-H. Lee, N. Park, M. Suh, W.-S. Chae, J. Cao, X. Peng, H. Jung, C. Kang, J. S. Kim, 'A Self-Calibrating Bipartite Viscosity Sensor for Mitochondria', *J. Am. Chem. Soc.* **2013**, *135*, 9181 – 9185.
[64] M. Dakanali, T. H. Do, A. Horn, A. Chongchivivat, T. Jarusreni, D. Lichlyter, G. Guizzunti, M. A. Haidekker, E. A. Theodorakis, 'Self-Calibrating Viscosity Probes: Design and Subcellular Localization', *Bioorg. Med. Chem.* **2012**, *20*, 4443 – 4450.
[65] Y. Niko, P. Didier, Y. Mely, G. Konishi, A. S. Klymchenko, 'Bright and Photostable Push-Pull Pyrene Dye Visualizes Lipid Order Variation between Plasma and Intracellular Membranes', *Sci. Rep.* **2016**, *6*, 18870.

[66] C. R. Woodford, E. P. Frady, R. S. Smith, B. Morey, G. Canzi, S. F. Palida, R. C. Araneda, W. B. Kristan Jr, C. P. Kubiak, E. W. Miller, R. Y. Tsien, 'Improved PeT Molecules for Optically Sensing Voltage in Neurons', *J. Am. Chem. Soc.* **2015**, *137*, 1817 – 1824.
[67] E. W. Miller, J. Y. Lin, E. P. Frady, P. A. Steinbach, W. B. Kristan Jr, R. Y. Tsien, 'Optically Monitoring Voltage in Neurons by Photo-Induced Electron Transfer through Molecular Wires', *Proc. Natl. Acad. Sci. U.S.A.* **2012**, *109*, 2114 – 2119.
[68] P. Yan, A. Xie, M. Wei, L. M. Loew, 'Amino(oligo)thiophene-Based Environmentally Sensitive Biomembrane Chromophores', *J. Org. Chem.* **2008**, *73*, 6587 – 6594.
[69] M. Macchione, N. Chuard, N. Sakai, S. Matile, 'Planarizable Push-Pull Probes: Overtwisted Flipper Mechanophores', *ChemPlusChem* **2017**, *29*, 1062 – 1066.
[70] P. Morelli, E. Bartolami, N. Sakai, S. Matile, 'Glycosylated Cell-Penetrating Poly(disulfide)s: Multifunctional Cellular Uptake at High Solubility', *Helv. Chim. Acta* **2018**, *101*, e1700266.
[71] P. Morelli, S. Matile, 'Sidechain Engineering in Cell-Penetrating Poly(disulfide)s', *Helv. Chim. Acta* **2017**, *100*, e1600370.
[72] N. Sakai, D. Houdebert, S. Matile, 'Voltage-Dependent Formation of Anion Channels by Synthetic Rigid-Rod Push-Pull Barrels', *Chem. Eur. J.* **2003**, *9*, 223 – 232.
[73] A. Vargas Jentzsch, D. Emery, J. Mareda, S. K. Nayak, P. Metrangolo, G. Resnati, N. Sakai, S. Matile, 'Transmembrane Anion Transport Mediated by Halogen-Bond Donors', *Nat. Commun.* **2012**, *3*, 905.
[74] B. Walker, M. Krishnasastry, L. Zorn, J. Kasianowicz, H. Bayley, 'Functional Expression of the alpha-Hemolysin of *Staphylococcus aureus* in Intact *Escherichia coli* and Cell Lysates. Deletion of Five C-Terminal Amino Acids Selectively Impairs Hemolytic Activity', *J. Biol. Chem.* **1992**, *267*, 10902 – 10909.
[75] P. Läuger, 'Mechanisms of Biological Ion Transport – Carriers, Channels, and Pumps in Artificial Lipid Membranes', *Angew. Chem. Int. Ed.* **1985**, *24*, 905 – 923.
[76] N. Sakai, Y. Kamikawa, M. Nishii, T. Matsuoka, T. Kato, S. Matile, 'Dendritic Folate Rosettes as Ion Channels in Lipid Bilayers', *J. Am. Chem. Soc.* **2006**, *128*, 2218 – 2219.
[77] O. S. Smart, J. Breed, G. R. Smith, M. S. P. Sansom, 'A Novel Method for Structure-Based Prediction of Ion Channel Conductance Properties,' *Biophys. J.* **1997**, *72*, 1109 – 1126.
[78] B. Hille, 'Ionic Channels of Excitable Membranes', 3rd Edn., Sinauer, Sunderland, MA, 2001.
[79] S. Futaki, D. Noshiro, T. Kiwada, K. Asami, 'Extramembrane Control of Ion Channel Peptide Assemblies, Using Alamethicin as an Example', *Acc. Chem. Res.* **2013**, *46*, 2924 – 2933.
[80] A. Perez-Velasco, V. Gorteau, S. Matile, 'Rigid Oligoperylenediimide Rods: Anion-π Slides with Photosynthetic Activity', *Angew. Chem. Int. Ed.* **2008**, *47*, 921 – 923.

Received February 9, 2018
Accepted March 20, 2018

